European Journal of Medicinal Chemistry 48 (2012) 132–142

Contents lists available at SciVerse ScienceDirect

European Journal of Medicinal Chemistry

journal homepage: http://www.elsevier.com/locate/ejmech

Original article

Cobalt(II) complexes with non-steroidal anti-inflammatory drug tolfenamic acid: Structure and biological evaluation

Sofia Tsiliou [a], Lida-Aikaterini Kefala [a], Franc Perdih [b], Iztok Turel [b], Dimitris P. Kessissoglou [a], George Psomas [a,*]

[a] Department of General and Inorganic Chemistry, Faculty of Chemistry, Aristotle University of Thessaloniki, GR-54124 Thessaloniki, Greece
[b] Faculty of Chemistry and Chemical Technology, University of Ljubljana, Askerceva 5, 1000 Ljubljana, Slovenia

ARTICLE INFO

Article history:
Received 20 October 2011
Received in revised form
28 November 2011
Accepted 3 December 2011
Available online 9 December 2011

Keywords:
Non-steroidal anti-inflammatory drugs
Tolfenamic acid
Cobalt(II) complexes
Crystal structures
Interaction with calf-thymus DNA
Interaction with albumins

ABSTRACT

Cobalt(II) complexes with the non-steroidal anti-inflammatory drug tolfenamic acid in the presence or absence of nitrogen-donor heterocyclic ligands (2,2′-bipyridine, 1,10-phenanthroline, 2,2′-bipyridylamine or pyridine) have been synthesized and characterized with physicochemical and spectroscopic techniques. The deprotonated tolfenamato ligands are coordinated to Co(II) ion through carboxylato oxygen atoms. The crystal structures of complexes [bis(2,2′-bipyridine) bis(methanol)bis(tolfenamato)cobalt(II)] **2** and [bis(2,2′-bipyridylamine)bis(tolfenamato)cobalt(II)] **4** have been determined by X-ray crystallography. UV studies of the interaction of the complexes with calf-thymus DNA (CT DNA) have shown that the complexes can bind to CT DNA and [bis(methanol)(1,10-phenanthroline)bis(tolfenamato)cobalt(II)] exhibits the highest binding constant to CT DNA. The cyclic voltammograms of the complexes recorded in DMSO solution and in the presence of CT DNA in 1/2 DMSO/buffer (containing 150 mM NaCl and 15 mM trisodium citrate at pH 7.0) solution have shown that they can bind to CT DNA by the intercalative binding mode which has also been verified by DNA solution viscosity measurements. Competitive study with ethidium bromide (EB) has shown that the complexes can displace the DNA-bound EB indicating that they bind to DNA in strong competition with EB. Tolfenamic acid and its cobalt(II) complexes exhibit good binding propensity to human or bovine serum albumin protein having relatively high binding constant values.

1. Introduction

Cobalt is an element of biological interest and its role is mainly focused on its presence in the active center of vitamin B12, which regulates indirectly the synthesis of DNA [1]. Additionally, cobalt is involved in the co-enzyme of vitamin B12 used as a supplement of the vitamin [2] and at least eight cobalt-dependent proteins have been reported [1]. Since the first reported studies into the biological activity of Co complexes [3] in 1952, diverse structurally characterized cobalt complexes have been studied as hydrolytic agents for DNA cleavage [4] and others showing antitumor–antiproliferative [5–7], antimicrobial [8–10], antifungal [11,12], antiviral [13,14] and antioxidant [15,16] activity have been reported.

Non-steroidal anti-inflammatory drugs (= NSAIDs) are among the most frequently used medicinal drugs used as analgesic, anti-inflammatory and antipyretic agents [17]. NSAIDs can act by inhibiting the cyclo-oxygenase(= COX)-mediated production of prostaglandins or via COX-independent mechanisms by modulating cell proliferation and cell death in cultured colon cancer cells lacking COX [18,19]. They have also exhibited anti-tumorigenic activity by reducing the number and size of carcinogen-induced colon tumors and a synergistic role on the activity of certain anti-tumor drugs, although the mechanism has not been completely clarified [20,21]. Therefore, the direct interaction of NSAIDs and their metal complexes with DNA is of interest since their anticancer as well as the anti-inflammatory activity may be explained [22,23]. In addition, it has been reported that the metal complexes of some NSAIDs are more active than their parent compounds [15,24,25].

Abbreviations: b, broad; bipy, 2,2′-bipyridine; bipyam, 2,2′-bipyridylamine; BSA, bovine serum albumin; COX, cyclooxygenase; CT, calf-thymus; DMF, *N*,*N*-dimethylformamide; DMSO, dimethylsulfoxide; EB, ethidium bromide (=3,8-diamino-5-ethyl-6-phenyl-phenanthridinium bromide); HSA, human serum albumin; Htolf, tolfenamic acid (= 2-[(3-chloro-2-methylphenyl)amino]benzoic acid); m, medium; NSAID, non-steroidal anti-inflammatory drug; phen, 1,10-phenanthroline; py, pyridine; *r*, [compound]/[CT DNA] mixing ratios; s, strong; SA, serum albumin; TEAP, tetraethylammonium perchlorate; vs, very strong.

* Corresponding author. Tel.: +30 2310997790; fax: +30 2310997738.
E-mail address: gepsomas@chem.auth.gr (G. Psomas).

0223-5234/$ – see front matter © 2011 Elsevier Masson SAS. All rights reserved.
doi:10.1016/j.ejmech.2011.12.004

Phenylalkanoic acids, anthranilic acids, oxicams, salicylate derivatives, sulfonamides and furanones are the main chemical classes of NSAIDs [26]. The NSAID tolfenamic acid (= Htolf, Scheme 1) belongs to the derivatives of *N*-phenylanthranilic acid and resembles chemically to mefenamic and niflumic acid and other fenamates in clinical use [26]. Htolf is found in analgesic, anti-inflammatory, antipyretic and antirheumatoid drugs and is also used for veterinary purposes [27]. A thorough survey of the literature has revealed the crystal structures of two tin(IV) complexes [28] and a copper(II) complex [29]. To the best of our knowledge, the only cobalt(II) complexes with NSAIDs of the anthranilic acids' group as ligands are two mefenamato ones recently reported by our lab [15].

Our recent research studies have been focused on the interaction of carboxylate-containing antimicrobial [30–36] or anti-inflammatory [15,16,37–40] agents with metal ions (Co^{2+}, Ni^{2+}, Cu^{2+}, Zn^{2+}) in an attempt to examine their mode of binding and possible biological relevance. In addition, we have reported studies on the interaction of the resultant metal complexes with biomolecules (nucleic acids and serum albumin proteins) and their potential biological (antimicrobial, anticancer, antioxidant) activity.

Taking into consideration the biological role and activity of cobalt and its complexes as well as the significance of the NSAIDs in medicine, we have initiated the investigation of the interaction of cobalt(II) with the NSAIDs mefenamic acid and naproxen as ligands [15,16]. In this context, we report the synthesis, the structural characterization, the electrochemical and the biological properties of the neutral mononuclear cobalt(II) complexes with the NSAID tolfenamic acid in the absence ($[Co(tolf)_2(MeOH)_4]$ **1**) or presence of a nitrogen-donor heterocyclic ligand such as 2,2′-bipyridine (= bipy), 1,10-phenanthroline (= phen), 2,2′-bipyridylamine (= bipyam) or pyridine (= py) ($[Co(tolf)_2(bipy)(MeOH)_2]$ **2**, $[Co(tolf)_2(phen)(MeOH)_2]$ **3**, $[Co(tolf)_2(bipyam)]$ **4** and $[Co(tolf)_2(py)_2(MeOH)_2]$ **5**, respectively). The crystal structures of **2** and **4** have been determined by X-ray crystallography. The investigation of the biological properties of Htolf and its complexes has been focused on (i) the affinity for bovine (BSA) and human serum albumin (HSA) proteins involved in the transport of metal ions and metal complexes with drugs through the blood stream, performed by fluorescence spectroscopy and (ii) the binding properties with calf-thymus (CT) DNA performed by UV spectroscopy, DNA solution viscosity measurements, cyclic voltammetry and competitive binding studies with ethidium bromide (= EB). Additionally, these biological properties have been evaluated in comparison to those of the Co(II) mefenamato and naproxenato complexes recently reported by our lab [15,16].

2. Results and discussion

2.1. Synthesis and characterization of the complexes

The synthesis of the complexes in high yield was achieved via the aerobic reaction of tolfenamic acid ($C_{13}H_{11}ClN$–COOH, Htolf) and KOH with $CoCl_2{\cdot}6H_2O$ in the absence, (eq. (1)) for **1**, or presence of the corresponding N-donor heterocyclic ligand, e.g. (bipy, eq. (2)) for **2** and (bipyam, eq. (3)) for **4** according to the equations:

$$CoCl_2{\cdot}6H_2O + 2Htolf + 2KOH + 4CH_3OH \rightarrow [Co(tolf)_2(CH_3OH)_4] + 2KCl + 8H_2O \quad (1)$$

$$CoCl_2{\cdot}6H_2O + 2Htolf + 2KOH + bipy + 2CH_3OH \rightarrow [Co(tolf)_2(bipy)(CH_3OH)_2] + 2KCl + 8H_2O \quad (2)$$

$$CoCl_2{\cdot}6H_2O + 2Htolf + 2KOH + bipyam \rightarrow [Co(tolf)_2(bipyam)] + 2KCl + 8H_2O \quad (3)$$

The complexes are soluble in DMSO and stable in the air. The molar conductivity values (Λ_M) of 1 mM DMSO solution of the complexes fall in the range 5–13 mho cm^2 mol^{-1} indicating that there is not any significant dissociation and the complexes are non-electrolytes in DMSO solution.

IR spectroscopy may be used in order to confirm the deprotonation and binding mode of tolfenamic acid. In the IR spectrum of Htolf, the observed absorption band at 3355(b (= broad), m (= medium)) cm^{-1}, attributed to the ν(H–O) stretching vibration has disappeared upon binding to the metal ion. The bands at 1661(s (= strong)) cm^{-1} and 1265(s) cm^{-1} attributed to the stretching vibrations $\nu(C{=}O)_{carboxylic}$ and $\nu(C{-}O)_{carboxylic}$ of the carboxylic moiety (–COOH) respectively, have shifted in the IR spectra of complexes **1**–**5**, in the range 1573–1583 cm^{-1} and 1377–1402 cm^{-1} assigned to antisymmetric, $\nu_{asym}(C{=}O)$, and symmetric, $\nu_{sym}(C{=}O)$, stretching vibrations of the carboxylato group, respectively. The difference Δ [$= \nu_{asym}(C{=}O) - \nu_{sym}(C{=}O)$], a useful characteristic tool for determining the coordination mode of the carboxylato ligands, gives a value falling in the range 195–204 cm^{-1} for complexes **1**–**3** and **5** indicative for an asymmetrically binding mode of the tolfenamato ligand [41], while for complex **4** the Δ value of 171 cm^{-1} may suggest a bidentate mode of the tolfenamato ligand [15].

The UV–Vis spectra of the complexes have been recorded as nujol mull and in DMSO solution and are similar suggesting that the complexes retain their structure in solution. In the visible region, three low-intensity bands are observed and can be assigned to d-d transitions. More specifically, for local O_h symmetry, band I observed in the region 680–742 nm ($\varepsilon = 10$–15 M^{-1} cm^{-1}) may be attributed to a $^4T_{1g}(F) \rightarrow {}^4T_{2g}$ transition, band II in the region 540–565 nm ($\varepsilon = 25$–60 M^{-1} cm^{-1}) to a $^4T_{2g}(F) \rightarrow {}^4A_{2g}$ transition and band III at 470–485 nm ($\varepsilon = 25$–40 M^{-1} cm^{-1}) to a $^4T_{1g}(F) \rightarrow {}^4T_{1g}(P)$ transition and are typical for distorted octahedral high-spin Co^{2+} complexes [1]. Additionally, an absorption band assigned to charge transfer transition exists at 385–395 nm ($\varepsilon = 210$–290 M^{-1} cm^{-1}).

In order to investigate the stability of the complexes in solution, the UV–Vis spectra of DMSO solutions of the complexes were recorded in the concentration range 0.5–10 mM. These solutions were prepared by dilution of the 10 mM DMSO solution. In the plots of the absorbance on the λ_{max} (A_{max}) vs the concentration for the complexes' solution (Figure S1), the experimental data are line-fitted (>99%) according to Beer's law suggesting that there is no significant dissociation.

The UV spectra of the complexes have been also recorded in the pH range 6–8 (since the biological experiments are performed at pH = 7) with the use of diverse buffer solutions (150 mM NaCl and 15 mM trisodium citrate at pH values regulated by HCl solution) and no significant changes (shift of the λ_{max} or new peaks) occurred (Figure S2), indicating that the complexes are stable in the pH range 6–8. The fact that complexes **1**–**5** are non-electrolytes in DMSO

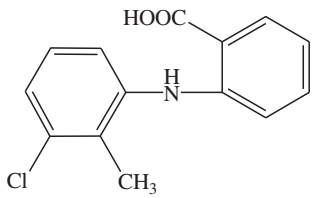

Scheme 1. Tolfenamic acid (Htolf = 2-[(3-chloro-2-methylphenyl)amino]benzoic acid).

solution and they have the same UV–Vis spectral pattern in nujol and in DMSO solution as well as in the presence of the buffer solution (150 mM NaCl and 15 mM trisodium citrate in the pH = 7.0) used in the biological experiments and in the pH range = 6–8 suggests that the compounds are stable and keep their integrity in solution.

The observed values of μ_{eff} (=4.25–4.75 BM) for the complexes at room temperature are higher than the spin-only value (=3.87 BM) showing spin-orbit coupling due to $t_{2g}^5e_g^2$ electron configuration. The values are within the range reported for mononuclear high-spin Co(II) complexes ($S = 3/2$) [1].

2.2. Structure of the complexes

2.2.1. Crystal structure of $[Co(tolf)_2(bipy)(MeOH)_2]$, **2**

A diagram of **2** is shown in Fig. 1, and selected bond distances and angles are listed in Table 1. The complex is mononuclear and the tolfenamato ligand behaves as a monodentate deprotonated ligand coordinated to cobalt atom via a carboxylate oxygen.

The cobalt atom is six-coordinate and is surrounded by two monodentate tolfenamato ligands, two methanol molecules and a bidentate 2,2′-bipyridine ligand showing a distorted octahedral geometry. The two nitrogen atoms of bipy and two oxygen atoms of the methanol molecules form the basal plane of the octahedron with the two oxygen atoms from the tolfenamato ligands lying at the apical.

The bond distances around cobalt atom are not equal, with the coordinated carboxylate oxygen atoms (Co(1)–O(1) = 2.0565(17) Å) lying closer to Co than the methanol oxygens (Co(1)–O(3) = 2.084(3) Å) and the bipy nitrogens (Co–N(2)) being at a distance 2.128(3) Å. The methanol molecules are lying at *cis* positions (O(31)–Co–O(31)' = 91.6(3)°) and the tolfenamato oxygens are *trans* (O(2)–Co–O(2)' = 179.71(15)°) to each other. The carboxylate group is asymmetrically bound to cobalt (C(1)–O(2) = 1.251(3) Å and C(1)–O(1) = 1.247(3) Å).

The N(2)–Co(1)–N(2)' angle observed is 76.67(15)° and is similar to reported values of other chelating polycyclic diimines [30–40]. The 2,2′-bipyridine ligand is planar with the cobalt atom lying in this plane.

2.2.2. Crystal structure of $[Co(tolf)_2(bipyam)]$, **4**

A diagram of **4** is shown in Fig. 2, and selected bond distances and angles are listed in Table 2. The complex is mononuclear and the tolfenamato ligands behave as deprotonated bidentate ligands coordinated to cobalt atom via the carboxylato groups which adopt

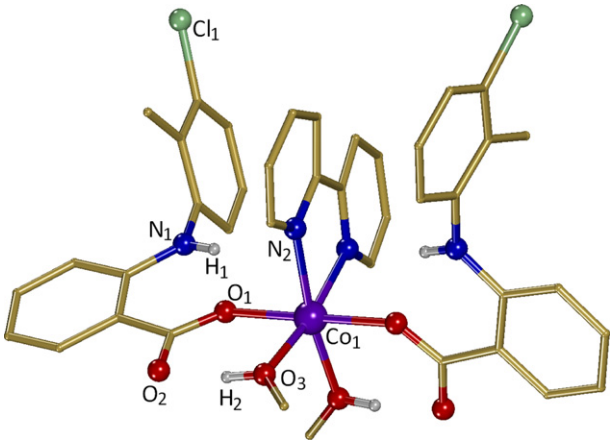

Fig. 1. A drawing of the molecular structure of **2** with only the heteroatoms labeling.

Table 1
Selected bond distances and angles for **2**.

Bond	Distance (Å)	Bond	Distance (Å)
Co(1)–O(1)	2.0565(17)	C(1)–O(1)	1.251(3)
Co(1)–O(3)	2.084(3)	C(1)–O(2)	1.247(3)
Co(1)–N(2)	2.128(3)	–	–
Angle	**(°)**	**Angle**	**(°)**
O(1)–Co(1)–O(1)'	179.71(15)	O(1)'–Co(1)–O(3)	91.94(11)
O(1)–Co(1)–O(3)	88.27(10)	O(1)'–Co(1)–O(3)'	88.27(10)
O(1)–Co(1)–N(2)	87.28(9)	O(1)'–Co(1)–N(2)	92.49(11)
O(1)–Co(1)–O(3)'	91.94(11)	O(1)'–Co(1)–N(2)'	87.28(9)
O(1)–Co(1)–N(2)'	92.49(11)	O(3)–Co(1)–O(3)'	91.6(3)
O(3)'–Co(1)–N(2)	96.04(15)	O(3)–Co(1)–N(2)	171.28(15)
O(3)'–Co(1)–N(2)'	171.28(15)	O(3)–Co(1)–N(2)'	96.04(15)
N(2)–Co(1)–N(2)'	76.67(15)	–	–

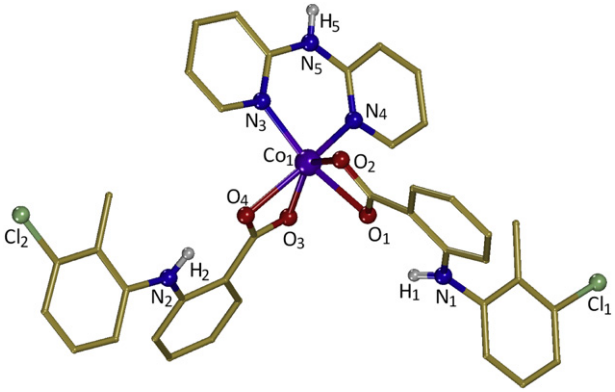

Fig. 2. A drawing of the molecular structure of **4** with only the heteroatoms labeling.

the asymmetric chelating mode (C(1)–O(1) = 1.266(2) Å and C(1)–O(2) = 1.275(2) Å, C(15)–O(3) = 1.271(2) Å and C(15)–O(4) = 1.274(2) Å).

In **4**, the cobalt atom is six-coordinate and is surrounded by two tolfenamato ligands and a bidentate 2,2′-bipyridylamine ligand showing a distorted trigonal prismatic geometry with the six vertices occupied by two nitrogen and four oxygen atoms, giving a CoN_2O_4 chromophore. More specifically, the plane of each trigonal base of the trigonal prism is formed by a nitrogen atom of bipyam and two oxygen atoms from the two tolfenamato ligands. N(4), O(1) and O(4) form the one base (base 1) of the prism and N(3), O(2) and O(3) form the second base (base 2). The two trigonal basal planes form an angle of 17.47° and lie at mean distance of

Table 2
Selected bond distances and angles for **4**.

Bond	Distance (Å)	Bond	Distance (Å)
Co(1)–O(3)	2.0566(12)	Co(1)–O(4)	2.223(1)
Co(1)–N(3)	2.0667(14)	C(1)–O(1)	1.266(2)
Co(1)–N(4)	2.0705(14)	C(1)–O(2)	1.275(2)
Co(1)–O(1)	2.1772(12)	C(15)–O(3)	1.271(2)
Co(1)–O(2)	2.1956(12)	C(15)–O(4)	1.274(2)
Angle	**(°)**	**Angle**	**(°)**
O(1)–Co(1)–O(2)	59.85(4)	O(2)–Co(1)–O(3)	137.13(5)
O(1)–Co(1)–O(3)	84.53(5)	O(2)–Co(1)–O(4)	96.10(5)
O(1)–Co(1)–O(4)	94.45(5)	O(2)–Co(1)–N(3)	93.93(5)
O(1)–Co(1)–N(3)	153.58(5)	O(2)–Co(1)–N(4)	107.47(5)
O(1)–Co(1)–N(4)	94.32(5)	O(3)–Co(1)–O(4)	61.35(4)
O(4)–Co(1)–N(3)	91.43(5)	O(3)–Co(1)–N(3)	120.58(5)
O(4)–Co(1)–N(4)	156.16(5)	O(3)–Co(1)–N(4)	97.55(5)
N(3)–Co(1)–N(4)	90.50(5)	–	–

2.267 Å. The distances of the cobalt atom to the two bases are equal (Co(1)…base 1 = 1.161 Å and Co(1)…base 2 = 1.159 Å).

The bond distances around Co atom are not equal; two sets of bonds distances may be observed with the bipy nitrogen atoms N(3) and N(4) and the carboxylate oxygen O(3) being closer to Co (Co(1)–O(3) = 2.0566(12) Å, Co(1)–N(3) = 2.0667(14) Å and Co(1)–N(4) = 2.0705(14) Å) than the carboxylate oxygen atoms O(1), O(2) and O(4) (Co(1)–O(1) = 2.1772(12) Å, Co(1)–O(2) = 2.1956(12) Å and Co(1)–O(4) = 2.223(1) Å).

The N(3)–Co(1)–N(4) angle observed is 90.50(5)° and is similar to reported values of other chelating bipyam complexes [36].

The amino group of tolfenamic ligand in **2** and **4** and the methanol ligand in **2** are involved in intramolecular hydrogen bonding with the carboxylic group (Table S1). Crystal structure of **2** is further stabilized by weak C–H···O and C–Cl···*Cg*(arene) interactions. The compound **4** crystallizes as a centrosymmetric hydrogen-bonded dimers facilitated by N5–H5···O2^{i} interactions involving the amino group of bipyam ligand and carboxylic group of adjacent molecules (Table S1). Dimers are further stabilized by π–π interactions with *Cg*1···*Cg*2^{i} distance of 3.5474(10) Å [*Cg*1 and *Cg*2 are N3/C29–C33 and N4/C34–C38 ring centroids, respectively; symmetry code: (i) 1 − x, 1 − y, 1 − z] (Figure S3). Supramolecular aggregation of **4** is formed by a network of C–H···O, C–H···*Cg*(arene), C–Cl···*Cg*(arene) and π–π interactions with *Cg*2···*Cg*4^{ii} and *Cg*5···*Cg*5^{iii} centroid-to-centroid distances 3.7574(11) and 3.5690(11) Å, respectively [*Cg*4 and *Cg*5 are C8–C13 and C16–C21 ring centroids, respectively; symmetry codes: (ii) 1 − x, −y, 1 − z; (iii) 1 − x, − y, 2 − z] (Figures S4 and S5).

2.2.3. *Proposed structures for complexes **1**, **3** and **5***

Based on the experimental data (IR and UV–Vis spectroscopy, molar conductivity and magnetic measurements) and after a comparison with the existing structurally characterized Co(II)–NSAID complexes, we may propose a structure for complexes **1**, **3** and **5**. Therefore, complex **1** is expected to have similar structure with complex [Co(mefenamato)$_2$(MeOH)$_4$] [15] exhibiting an octahedral geometry with the NSAID ligand being coordinated to cobalt via a carboxylate oxygen atom. Complex **3** is expected to have similar structure to **2** presenting a distorted octahedral geometry with two monodentate NSAID ligands, a bidentate phen ligand and two coordinated methanol molecules. Additionally, complex **5** is expected to have similar structure to complex [Co(naproxenato)$_2$(py)$_2$(H$_2$O)$_2$] [16] which presents a distorted octahedral geometry with two monodentate NSAID ligands, two pyridine ligands and two coordinated aqua molecules.

2.3. Binding of the complexes to serum albumins

The study of the interaction of drugs and their compounds with blood plasma proteins and especially with serum albumin, which is the most abundant protein in plasma and is involved in the transport of metal ions and metal complexes with drugs through the blood stream, is of increasing interest. Binding to these proteins may lead to loss or enhancement of the biological properties of the original drug, or provide paths for drug transportation [42]. Bovine serum albumin (BSA) is the most extensively studied serum albumin, due to its structural homology with human serum albumin (HSA). HSA (one Trp-214) and BSA (containing two tryptophans, Trp-134 and Trp-212) solutions exhibit a strong fluorescence emission with a peak at 351 nm and 343 nm, respectively, due to the tryptophan residues, when excited at 295 nm [43]. The interaction of Htolf and complexes **1**–**5** with serum albumins has been studied from tryptophan emission-quenching experiments. The changes in the emission spectra of tryptophan in BSA or HSA are primarily due to change in protein conformation, subunit association, substrate binding or denaturation. Tolfenamic acid and complexes **1**–**5** exhibited a maximum emission at 330 nm under the same experimental conditions and the SA fluorescence spectra have been corrected before the experimental data processing [15].

Addition of tolfenamic acid or its complexes **1**–**5** to HSA results in relatively moderate fluorescence quenching (up to 44% of the initial fluorescence intensity of HSA for Htolf, 41% for **1**, 81% for **2**, 42% for **3**, 46% for **4** and 57% for **5**, as calculated after the correction of the initial fluorescence spectra) (Fig. 3(A)), due to possible changes in protein secondary structure of HSA indicating the binding of the compounds to HSA [44].

The Stern–Volmer and Scatchard graphs may be used in order to study the interaction of a quencher with serum albumins. According to Stern–Volmer quenching equation [15,35]:

$$\frac{I_0}{I} = 1 + k_q\tau_0[Q] = 1 + K_{SV}[Q] \quad (4)$$

where I_0 = the initial tryptophan fluorescence intensity of SA, I = the tryptophan fluorescence intensity of SA after the addition of the quencher, k_q = the quenching rate constants of SA, K_{SV} = the dynamic quenching constant, τ_o = the average lifetime of SA without the quencher, [Q] = the concentration of the quencher respectively,

$$K_{SV} = k_q\tau_0 \quad (5)$$

and, taking as fluorescence lifetime (τ_o) of tryptophan in SA at around 10^{-8} s, the dynamic quenching constant (K_{SV}, M^{-1}) can

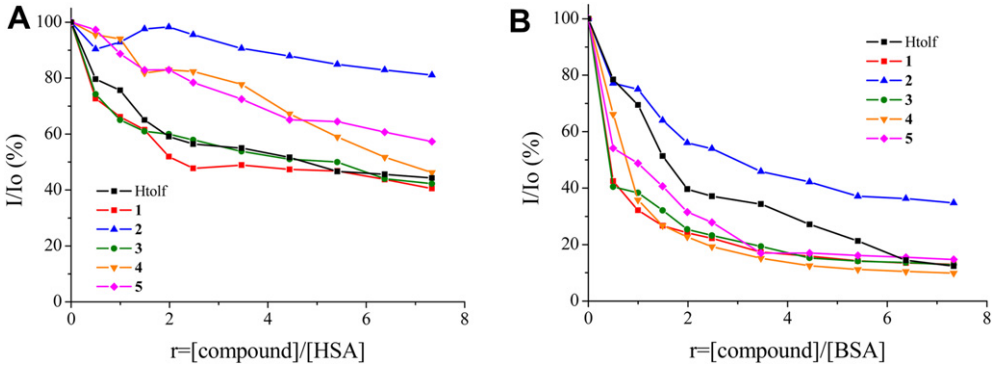

Fig. 3. (A) Plot of % relative fluorescence intensity at λ_{em} = 351 nm (I/I_0%) vs r (r = [compound]/[HSA]) for Htolf and complexes **1**–**5** in buffer solution (150 mM NaCl and 15 mM trisodium citrate at pH 7.0). (B) Plot of % relative fluorescence intensity at λ_{em} = 343 nm (I/I_0%) vs r (r = [compound]/[BSA]) for Htolf and complexes 1–5 in buffer solution (150 mM NaCl and 15 mM trisodium citrate at pH 7.0).

be obtained by the slope of the diagram I_0/I vs [Q] (Figure S6), and subsequently the approximate quenching constant (k_q, M^{-1} s^{-1}) may be calculated. The calculated values of K_{sv} and k_q for the interaction of the compounds with HSA are given in Table 3 and indicate good HSA binding propensity of the compounds with Htolf and **1** exhibiting the highest HSA quenching ability. The k_q values ($<1 \times 10^{12}$ M^{-1} s^{-1}) are higher than diverse kinds of quenchers for biopolymers fluorescence (2.0×10^{10} M^{-1} s^{-1}) indicating the existence of static quenching mechanism.

Using the Scatchard equation [15]:

$$\frac{\Delta I/I_0}{[Q]} = nK - K\frac{\Delta I}{I_0} \quad (6)$$

where n is the number of binding sites per albumin and K is the association binding constant, K (M^{-1}), may be calculated from the slope in plots $\Delta I/I_0/[Q]$ versus $\Delta I/I_0$ (Figure S7) and n is given by the ratio of y intercept to the slope [15]. It is obvious (Table 3) that the coordination of Htolf to Co(II) results in an increased K value for HSA with complex **1** exhibiting the highest K value among the compounds while the co-existence of a N-donor ligand results in a decreased affinity for HSA. Additionally, the n value of Htolf increases when it is coordinated to Co(II) in the presence of bipyam or py.

The quenching provoked by Htolf or tolfenamato complexes **1**–**5** to the BSA fluorescence (Fig. 3(B)) is much more pronounced than the corresponding HSA quenching (up to 12% of the initial BSA fluorescence intensity for Htolf, 13% for **1**, 35% for **2**, 13% for **3**, 10% for **4** and 15% for **5**) indicating that the binding of each compound to BSA quenches the intrinsic fluorescence of the tryptophans in BSA [43].

The Stern–Volmer equation applied for the interaction with BSA in Figure S8 shows that the curves have fine linear relationships ($r = 0.99$). The calculated values of K_{SV} and k_q are given in Table 3 and indicate their good BSA binding propensity with complex **4** exhibiting the highest BSA quenching ability. From the Scatchard graph (Figure S9), the association binding constant to BSA of each compound has been calculated (Table 3) with complexes exhibiting higher K values than free Htolf. The n value of Htolf presents a slight decrease when it is coordinated to Co(II) in complexes **1**–**5** (Table 3).

Comparing the affinity of complexes **1**–**5** for BSA and HSA (K values), it is obvious that complexes **1**–**5** show higher affinity for BSA than HSA, in contrast to Htolf which presents higher affinity for HSA. Additionally, complexes **1**–**5** exhibit higher binding affinity for BSA than their Co(II) mefenamato analogues, while for HSA complexes **1** and **3** present higher and **2**, **4** and **5** lower K values than their Co(II) mefenamato analogues [15].

2.4. Study of the interaction of the complexes with CT DNA with UV spectroscopy

Transition metal complexes can bind to DNA via both covalent (via replacement of a labile ligand of the complex by a nitrogen base of DNA) and/or noncovalent (intercalation, electrostatic or groove binding) interactions [15]. In the literature, metal complexes of the oxicam NSAIDs have been found to bind to DNA via the intercalative mode [45], while the interaction of DNA with the copper(II) complexes of naproxen, diclofenac (NSAIDs of the phenylalkanoic acids' group) and diflunisal (a salicylate derivative NSAID) as well as of cobalt(II) naproxenato or mefenamato complexes (mefenamic acid belongs to the group of the anthralinic acid NSAIDs) has been recently reported by our lab [15,16,38–40].

The UV spectra have been recorded for a constant CT DNA concentration in different [compound]/[DNA] mixing ratios (r) (compound = Htolf or **1**–**5**). UV spectra of CT DNA in the presence of a compound derived for diverse r values are shown representatively for **4** in Fig. 4(A). The band at $\lambda_{max} = 258$ nm exhibits a red-shift up to 266 nm for all compounds, indicating that the interaction with CT DNA results in the direct formation of a new complex with double-helical CT DNA [46] with a simultaneous stabilization of the CT DNA duplex [47].

In the UV spectra of the complexes, the intense absorption bands observed are attributed to the intra-ligand transitions of the coordinated groups of tolfenamato ligands. Any interaction between each complex and CT DNA that could perturb its intra-ligand centred spectral transitions during the titration upon addition of CT DNA in diverse r values can be observed [37]. In general, the changes observed in the UV spectra upon titration may give evidence of the existing interaction mode, since a hypochromism due to $\pi \rightarrow \pi^*$ stacking interactions may appear in the case of the intercalative binding mode, while red-shift (bathochromism) may be observed when the DNA duplex is stabilized [47].

In the UV spectrum of **5**, the band centred at 348 nm (band I) exhibits a significant hypochromism of 40% (Fig. 4(B)) suggesting tight binding to CT DNA probably by intercalation. Further addition of DNA results in a blue-shift with a gradual elimination of this band. Additionally, the band at 304 nm (band II) presents a hyperchromism of up to 19% accompanied by a red-shift of 5 nm (up to 309 nm), suggesting tight binding and stabilization. A distinct isosbestic point at 335 nm appears upon addition of CT DNA. The behaviour of Htolf (Fig. 4(C)) and complexes **1**–**4** upon addition of CT DNA is quite similar to **5**; for all compounds, the hypochromism of band I varies from 12% for **3** up to 60% for Htolf and the observed hyperchromism of band II is between 24% for **4** and 46% for **1** (Table 4).

The results derived from the UV titration experiments suggest that all the complexes can bind to CT DNA [30–36] although the

Table 3
The BSA and HSA binding constants and parameters (K_{sv}, k_q, K, n) derived for Htolf and complexes **1**–**5**.

	Compound	K_{SV} (M^{-1})	k_q (M^{-1} s^{-1})	K (M^{-1})	n
HSA	Htolf	$6.10(\pm0.38) \times 10^4$	$6.10(\pm0.38) \times 10^{12}$	$3.12(\pm0.25) \times 10^5$	0.63
	$[Co(tolf)_2(MeOH)_4]$	$5.71(\pm0.31) \times 10^4$	$5.71(\pm0.31) \times 10^{12}$	$4.62(\pm0.51) \times 10^5$	0.63
	$[Co(tolf)_2(bipy)(MeOH)_2]$	$1.15(\pm0.06) \times 10^4$	$1.15(\pm0.06) \times 10^{12}$	$3.40(\pm0.40) \times 10^4$	0.34
	$[Co(tolf)_2(phen)(MeOH)_2]$	$5.27(\pm0.28) \times 10^4$	$5.27(\pm0.28) \times 10^{12}$	$5.88(\pm0.45) \times 10^5$	0.54
	$[Co(tolf)_2(bipyam)]$	$5.04(\pm0.40) \times 10^4$	$5.04(\pm0.40) \times 10^{12}$	$2.20(\pm0.10) \times 10^4$	0.75
	$[Co(tolf)_2(py)_2(MeOH)_2]$	$3.40(\pm0.13) \times 10^4$	$3.40(\pm0.13) \times 10^{12}$	$5.74(\pm0.46) \times 10^4$	0.75
BSA	Htolf	$2.18(\pm0.12) \times 10^5$	$2.18(\pm0.12) \times 10^{13}$	$1.60(\pm0.14) \times 10^5$	1.11
	$[Co(tolf)_2(MeOH)_4]$	$2.88(\pm0.24) \times 10^5$	$2.88(\pm0.24) \times 10^{13}$	$1.11(\pm0.07) \times 10^6$	0.89
	$[Co(tolf)_2(bipy)(MeOH)_2]$	$8.60(\pm0.05) \times 10^4$	$8.60(\pm0.05) \times 10^{12}$	$1.39(\pm0.11) \times 10^5$	0.89
	$[Co(tolf)_2(phen)(MeOH)_2]$	$3.02(\pm0.21) \times 10^5$	$3.02(\pm0.21) \times 10^{13}$	$6.18(\pm0.24) \times 10^5$	0.94
	$[Co(tolf)_2(bipyam)]$	$4.30(\pm0.25) \times 10^5$	$4.30(\pm0.25) \times 10^{13}$	$6.68(\pm0.14) \times 10^5$	0.97
	$[Co(tolf)_2(py)_2(MeOH)_2]$	$2.74(\pm0.19) \times 10^5$	$2.74(\pm0.19) \times 10^{13}$	$3.65(\pm0.20) \times 10^5$	0.98

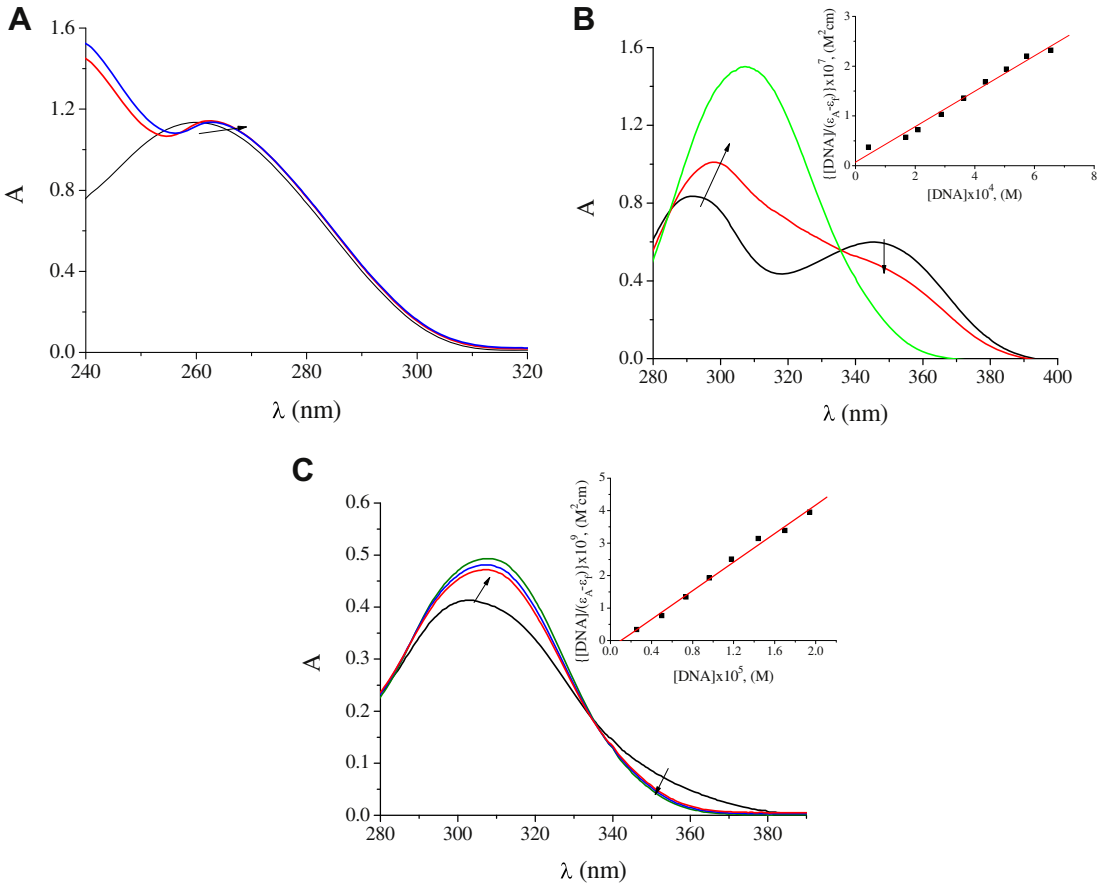

Fig. 4. (A) UV spectra of CT DNA in buffer solution (150 mM NaCl and 15 mM trisodium citrate at pH 7.0) in the absence or presence of [Co(tolf)$_2$(bipyam)] **4**. The arrows show the changes upon increasing amounts of the complex. (B) UV spectra of Htolf, in 1×10^{-5} M DMSO solution, in the presence of CT DNA at increasing amounts. (C) UV spectra of [Co(tolf)$_2$(py)$_2$(MeOH)$_2$] 5, in 1×10^{-5} M DMSO solution, in the presence of CT DNA at increasing amounts. The arrows in (B) and (C) show the changes upon increasing amounts of CT DNA. Insets in (B) and (C): plot of $[DNA]/(\varepsilon_A - \varepsilon_f)$ vs [DNA].

exact mode of binding cannot be merely proposed by UV spectroscopic titration studies. The existence of hypochromism could be considered as evidence that the binding of the complexes involving intercalation between the base pairs of CT DNA cannot be ruled out [30–36].

The binding constant of the complexes to CT DNA, K_b, is calculated by the ratio of slope to the *y* intercept in plots $[DNA]/(\varepsilon_A - \varepsilon_f)$ versus [DNA] (Insets in Fig. 4(B),(C)), according to the equation [47]:

$$\frac{[DNA]}{(\varepsilon_A - \varepsilon_f)} = \frac{[DNA]}{(\varepsilon_b - \varepsilon_f)} + \frac{1}{K_b(\varepsilon_b - \varepsilon_f)} \quad (7)$$

where [DNA] is the concentration of DNA in base pairs, $\varepsilon_A = A_{obsd}/[compound]$, ε_f = the extinction coefficient for the free compound and ε_b = the extinction coefficient for the compound in the fully bound form.

The calculated K_b values for Htolf and complexes **1**–**5** (Table 4) suggest a relatively strong binding of complexes **1**–**5** to CT DNA with complex **3** exhibiting the highest K_b value ($= 2.28(\pm 0.15) \times 10^6\ M^{-1}$). In comparison to the K_b values of the Co(II) mefenamato complexes, complexes **1**, **2** and **5** present similar or higher K_b values than their mefenamato analogues [15]. The K_b values of all complexes are close to that of the classical intercalator EB ($K_b = 1.23(\pm 0.07) \times 10^5\ M^{-1}$) [48].

2.5. Cyclic voltammetry and interaction with CT DNA

The cyclic voltammograms of **5** in DMSO solution exhibit a cathodic wave at −1020 mV (E_{pc1}) followed by two anodic waves at +10 mV (E_{pa1}) and at +680 mV (E_{pa2}). In the reverse scan, one more cathodic wave appears at −210 mV (E_{pc2}). The one-electron cathodic wave at E_{pc1} can be attributed to the reduction of

Table 4
The DNA binding constants (K_b) of Htolf and complexes **1**–**5**.

Compound	Band-I hypochromism (%)	Band-II hyperchromism (%)	K_b (M^{-1})
Htolf	60%	40%	$5.00(\pm 0.10) \times 10^4$
[Co(tolf)$_2$(MeOH)$_4$]	20%	46%	$1.14(\pm 0.20) \times 10^6$
[Co(tolf)$_2$(bipy)(MeOH)$_2$]	18%	28%	$4.18(\pm 0.40) \times 10^5$
[Co(tolf)$_2$(phen)(MeOH)$_2$]	12%	38%	$2.28(\pm 0.15) \times 10^6$
[Co(tolf)$_2$(bipyam)]	13%	24%	$6.78(\pm 0.50) \times 10^5$
[Co(tolf)$_2$(py)$_2$(MeOH)$_2$]	19%	40%	$9.77(\pm 0.25) \times 10^5$

[Co(II)] to [Co(I)], while the two anodic waves at E_{pa1} and E_{pa2} can be attributed to the oxidation processes [Co(I)] → [Co(II)] and [Co(II)] → [Co(III)], respectively, and the second cathodic wave at Ep_{c2} to the reduction of [Co(III)] to [Co(II)] species [15,16]. Complexes **1**–**4** present similar cyclic voltammograms in DMSO solution and the corresponding potentials are given in Table 5.

The electrochemical investigations of metal-DNA interactions may be a useful supplement to spectroscopic methods and provide information about interaction with both the reduced and oxidized form of the metal. In general, the electrochemical potential of a small molecule will shift positively when it intercalates into DNA double helix, and it will shift to a negative direction in the case of electrostatic interaction with DNA [15,33,34].

The quasi-reversible redox couple Co(II)/Co(I) for each complex in 1/2 DMSO/buffer solution has been studied upon addition of CT DNA and the corresponding potentials as well as their shifts are given in Table 6. No new redox peaks appeared after the addition of CT DNA to each complex, but the current intensity of all the peaks decreased significantly, suggesting the existence of an interaction between each complex and CT DNA, and can be explained in terms of an equilibrium mixture of free and DNA-bound complex to the electrode surface [49]. For increasing amounts of CT DNA, both the cathodic (E_{pc}) and the anodic potential (E_{pa}) for all complexes show a positive shift ($\Delta E_p = (-10) - (+35)$ mV) (Table 6) suggesting an intercalative mode of binding between the complexes and CT DNA [15,38–40,49].

2.6. DNA-binding study with viscosity measurements

DNA viscosity is sensitive to DNA length change and its measurement upon addition of a compound may be concerned as a reliable method to clarify the interaction mode of a compound with DNA, especially for the intercalative binding mode [50–52]. In the case of classic intercalation, DNA base pairs are separated in order to host the bound compound resulting in the lengthening of the DNA helix and subsequently increased DNA viscosity. On the other hand, the binding of a compound exclusively in DNA grooves by means of partial and/or non-classic intercalation causes a bend or kink in the DNA helix reducing slightly its effective length and, as a result, DNA solution viscosity is slightly decreased or remains unchanged [35,36,38–40,50–52].

Viscosity measurements were carried out on CT DNA solutions upon addition of increasing amounts of Htolf or complexes **1**–**5** (Fig. 5). Addition of complexes **1**–**5** resulted in a significant increase of the relative viscosity of DNA which can be explained by the insertion of the compounds in between the DNA base pairs, leading to an increase in the separation of base pairs at intercalation sites and, thus, an increase in overall DNA length. Therefore, intercalation of the complexes as the most possible interaction mode to CT DNA may be concluded.

2.7. Competitive study with ethidium bromide

Ethidium bromide (EB) is a typical indicator of intercalation since it can form soluble complexes with nucleic acids resulting in the emission of intense fluorescence due to the intercalation of the planar phenanthridine ring between adjacent base pairs on the double helix of CT DNA. The changes observed in the spectra of EB on its binding to CT DNA are often used for the interaction study between DNA and metal complexes [15,35].

Tolfenamic acid and complexes **1**–**5** show no fluorescence at room temperature in solution or in the presence of CT DNA, and their binding to DNA cannot be directly predicted through the emission spectra. Hence competitive EB binding studies may be undertaken in order to examine the binding of each compound with DNA since the fluorescence intensity is highly enhanced upon addition of CT DNA, due to its strong intercalation with DNA base pairs. Addition of a second molecule, which may bind to DNA more strongly than EB, results in a decrease the DNA-induced EB emission due to the replacement of EB, and/or electron transfer [33–36].

The emission spectra of EB bound to CT DNA in the absence and presence of each compound have been recorded for [EB] = 20 μM, [DNA] = 26 μM for increasing amounts of each compound. The addition of Htolf or each complex **1**–**5** at diverse *r* values (Fig. 6) results in a significant decrease of the intensity of the emission band of the DNA-EB system at 592 nm (up to 26% of the initial EB-DNA fluorescence intensity for Htolf and **2**, 27% for **1** and **4**, 21% for **3** and 22% for **5**) indicating the competition of the complexes with EB in binding to DNA. The observed significant quenching of DNA-EB fluorescence for Htolf and **1**–**5** suggests that they displace EB from the DNA-EB complex and they can probably interact with CT DNA by the intercalative mode [15,30–40].

The Stern–Volmer constant K_{SV} may be used to evaluate the quenching efficiency for each compound according to the equation:

$$\frac{I_0}{I} = 1 + K_{SV}[Q] \quad (8)$$

Table 5
Cathodic and anodic potentials (in mV) for the redox couples Co(II)/Co(I) (E_{pc1}, E_{pa1}) and Co(III)/Co(II) (E_{pc2}, E_{pa2}) in DMSO solution.

Complex	E_{pc1}	E_{pa1}	E_{pa2}	E_{pc2}
$[Co(tolf)_2(MeOH)_4]$	−1070	−40	+680	−180
$[Co(tolf)_2(bipy)(MeOH)_2]$	−1144	+40	+665	−195
$[Co(tolf)_2(phen)(MeOH)_2]$	−1120	+30	+675	−198
$[Co(tolf)_2(bipyam)]$	−1135	+65	+655	−205
$[Co(tolf)_2(py)_2(MeOH)_2]$	−1020	+10	+680	−210

Table 6
Cathodic and anodic potentials (in mV) for the redox couple Co(II)/Co(I) in 1/2 DMSO/buffer solution of the complexes in the absence and presence of CT DNA.

Complex	$E_{pc(f)}$ [a]	$E_{pc(b)}$ [b]	ΔE_{pc} [c]	$E_{pa(f)}$ [a]	$E_{pa(b)}$ [b]	ΔE_{pa} [c]
$[Co(tolf)_2(MeOH)_4]$	−800	−780	+20	−555	−565	−10
$[Co(tolf)_2(bipy)(MeOH)_2]$	−885	−850	+35	−530	−540	−10
$[Co(tolf)_2(phen)(MeOH)_2]$	−880	−860	+20	−575	−565	+10
$[Co(tolf)_2(bipyam)]$	−760	−750	+10	−555	−545	+10
$[Co(tolf)_2(py)_2(MeOH)_2]$	−780	−755	+25	−585	−575	−10

[a] $E_{pc/a}$ in DMSO/buffer in the absence of CT DNA ($E_{pc/a(f)}$).
[b] $E_{pc/a}$ in DMSO/buffer in the presence of CT DNA ($E_{pc/a(b)}$).
[c] $\Delta E_{pc/a} = E_{pc/a(b)} - E_{pc/a(f)}$.

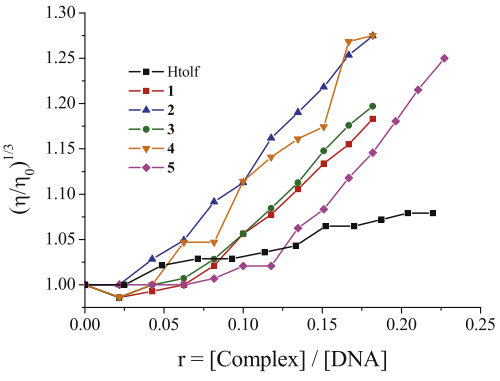

Fig. 5. Relative viscosity of CT DNA $(\eta/\eta_0)^{1/3}$ in buffer solution (150 mM NaCl and 15 mM trisodium citrate at pH 7.0) in the presence of Htolf and complexes **1**–**5** at increasing amounts (*r*).

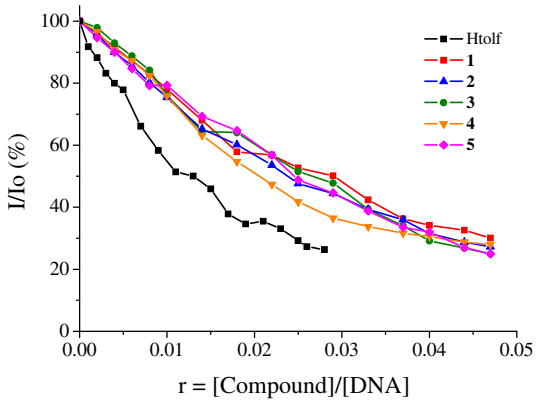

Fig. 6. Plot of EB relative fluorescence intensity at λ_{em} = 592 nm (I/I_0%) vs r (r = [compound]/[DNA]) for Htolf and complexes **1**–**5** in buffer solution (150 mM NaCl and 15 mM trisodium citrate at pH 7.0).

Table 7
EB-DNA fluorescence (%) and Stern–Volmer constants (K_{SV}) of Htolf complexes **1**–**5**.

Compounds	% of EB fluorescence (% I/I_0)	K_{sv} (M^{-1})
Htolf	26	$1.15(\pm0.04) \times 10^6$
$[Co(tolf)_2(MeOH)_4]$	27	$1.14(\pm0.05) \times 10^6$
$[Co(tolf)_2(bipy)(MeOH)_2]$	26	$1.26(\pm0.05) \times 10^6$
$[Co(tolf)_2(phen)(MeOH)_2]$	21	$1.51(\pm0.08) \times 10^6$
$[Co(tolf)_2(bipyam)]$	27	$1.31(\pm0.04) \times 10^6$
$Co(tolf)_2(py)_2(MeOH)_2]$	22	$1.41(\pm0.08) \times 10^6$

where I_0 and I are the emission intensities in the absence and the presence of the quencher, respectively, [Q] is the concentration of the quencher (Htolf or complexes **1**–**5**) and K_{SV} is obtained by the slope of the diagram I_0/I vs [Q]. The Stern–Volmer plots of DNA-EB for the compounds (Figure S10) illustrate that the quenching of EB bound to DNA by the compounds is in good agreement (R = 0.99) with the linear Stern–Volmer equation (eq. (8)), which proves that the replacement of EB bound to DNA by each compound results in a decrease in the fluorescence intensity. The high K_{SV} (Table 7) values of the compounds show that they can bind tightly to the DNA and are higher than those found for the Co(II) mefenamato complexes [15].

Table 8
Crystallographic data for complexes **2** and **4**.

	$[Co(tolf)_2(bipy)(MeOH)_2]$, **2**	$[Co(tolf)_2(bipyam)]$, **4**
Formula	$C_{40}H_{38}Cl_2CoN_4O_6$	$C_{38}H_{31}Cl_2CoN_5O_4$
Fw	800.57	751.51
T(K)	293(2)	150(2)
Crystal system	Orthorhombic	Triclinic
Space group	Ic2a	P-1
a(Å)	7.2590(2)	10.8126(2)
b(Å)	17.6131(4)	10.9511(2)
c(Å)	29.6327(7)	14.7192(3)
α(°)	90.00	83.1998(12)
β(°)	90.00	73.3966(13)
γ(°)	90.00	89.5768(13)
Volume (Å^3)	3788.64(16)	1657.84(5)
Z	4	2
D(calc), Mg m^{-3}	1.404	1.505
Abs. coef., μ, mm^{-1}	0.646	0.730
F(000)	1660	774
GOF on F^2	1.084	1.027
R1 [$I > 2\sigma$(I)]	0.0437[a]	0.0341[b]
wR2 [$I > 2\sigma$(I)]	0.1134[a]	0.0784[b]

[a] 3549 reflections with $I > 2\sigma$(I).
[b] 6284 reflections with $I > 2\sigma$(I).

3. Conclusions

The synthesis and characterization of the neutral mononuclear cobalt(II) complexes with the non-steroidal anti-inflammatory drug tolfenamic acid in the absence or presence of the nitrogen-donor heterocyclic ligands 2,2′-bipyridine, 1,10-phenanthroline, 2,2′-bipyridylamine or pyridine has been achieved. In these complexes, deprotonated tolfenamato ligand is bound to cobalt(II) via carboxylate oxygen atoms. Structurally characterized complexes $[Co(tolf)_2(bipy)(MeOH)_2]$ and $[Co(tolf)_2(bipyam)]$ present a distorted octahedral and trigonal prismatic geometry, respectively, around cobalt atom. Complexes **2** and **4** are among the few structurally characterized Co(II) complexes with NSAIDs as ligands.

UV spectroscopy, DNA solution viscosity measurements and cyclic voltammetry studies have revealed the ability of the complexes to bind to DNA. The binding strength of the compounds with CT DNA calculated with UV spectroscopic titrations have shown that the complexes present higher binding affinity to CT DNA than free tolfenamic acid with $[Co(tolf)_2(phen)(MeOH)_2]$ exhibiting the highest K_b value among the complexes examined. Cyclic voltammetry studies have confirmed the intercalation as the most possible binding mode to DNA and competitive binding studies with EB have revealed the ability of the complexes to displace EB from the EB-DNA complex.

The complexes show good binding affinity to BSA and HSA proteins giving relatively high binding constants.

Complexes **1**–**5** exhibit higher binding constants values to DNA and albumins than the corresponding Co(II) mefenamato complexes previously reported by our lab suggesting that tolfenamic acid could be considered a stronger binding ligand than mefenamic acid.

4. Experimental

4.1. Materials – instrumentation – physical measurements

All the chemicals ($CoCl_2 \cdot 6H_2O$, Htolf, bipy, phen, bipyam, py, KOH, CT DNA, BSA, HSA, EB, NaCl and trisodium citrate) were purchased from Sigma–Aldrich Co and all solvents were purchased from Merck. All the chemicals and solvents were reagent grade and were used as purchased without any further purification. Tetraethylammonium perchlorate (TEAP) was purchased from Carlo Erba and, prior to its use, it was recrystallized twice from ethanol and dried under vacuum.

DNA stock solution was prepared by dilution of CT DNA to buffer (containing 15 mM trisodium citrate and 150 mM NaCl at pH 7.0) followed by exhaustive stirring for three days, and kept at 4 °C for no longer than a week. The stock solution of CT DNA gave a ratio of UV absorbance at 260 and 280 nm (A_{260}/A_{280}) of 1.87, indicating that the DNA was sufficiently free of protein contamination. The DNA concentration was determined by the UV absorbance at 260 nm after 1:20 dilution using ε = 6600 M^{-1} cm^{-1} [15,38].

Infrared (IR) spectra (400–4000 cm^{-1}) were recorded on a Nicolet FT-IR 6700 spectrometer with samples prepared as KBr disk. UV–visible (UV–vis) spectra were recorded as nujol mulls and in solution at concentrations in the range 10^{-5}–10^{-3} M on a Hitachi U-2001 dual beam spectrophotometer. Room temperature magnetic measurements were carried out by the Faraday method using mercury tetrathiocyanatocobaltate(II) as a calibrant. C, H and N elemental analysis were performed on a Perkin–Elmer 240B elemental analyzer. Molar conductivity measurements were carried out with a Crison Basic 30 conductometer. Fluorescence spectra were recorded in solution on a Hitachi F-7000 fluorescence spectrophotometer.

Cyclic voltammetry studies were performed on an Eco chemie Autolab Electrochemical analyzer. Cyclic voltammetry experiments were carried out in a 30 mL three-electrode electrolytic cell. The working electrode was platinum disk, a separate Pt single-sheet electrode was used as the counter electrode and a Ag/AgCl electrode saturated with KCl was used as the reference electrode. The cyclic voltammograms of the complexes were recorded in 0.4 mM DMSO solutions and in 0.4 mM 1/2 DMSO/buffer solutions at $\nu = 100$ mV s^{-1} where TEAP and the buffer solution were the supporting electrolytes, respectively. Oxygen was removed by purging the solutions with pure nitrogen which had been previously saturated with solvent vapours. All electrochemical measurements were performed at 25.0 ± 0.2 °C.

4.2. Synthesis of the complexes

4.2.1. [Co(tolf)$_2$(MeOH)$_4$], **1**

A methanolic solution (15 mL) containing tolfenamic acid (0.5 mmol, 131 mg) and KOH (0.5 mmol, 28 mg) was stirred for 1 h. The solution was added to a methanolic solution (10 mL) of $CoCl_2 \cdot 6H_2O$ (0.25 mmol, 58.5 mg) and the reaction mixture was stirred for 1 h. The reaction solution was filtered and left for slow evaporation. Rose-colored microcrystalline product of [Co(tolf)$_2$(MeOH)$_4$], **1** (125 mg, 70%) was collected after a few days. *Anal.* Calcd. for $C_{32}H_{38}CoCl_2N_2O_8$ (MW = 708.50) C, 54.25; H, 5.41; N, 3.95%; found: C, 54.39; H, 5.40; N, 4.15%. IR: ν_{max}, cm^{-1}; $\nu_{asym}(CO_2)$, 1581 (vs (very strong)); $\nu_{sym}(CO_2)$, 1377 (vs); $\Delta = \nu_{asym}(CO_2) - \nu_{sym}(CO_2)$: 204 cm^{-1} (KBr disk); UV–vis: λ, nm (ε, M^{-1} cm^{-1}) as nujol mull: 735, 551, 490, 403, 339, 304; in DMSO: 742 (10), 563 (60), 478 (25), 395 (240), 343 (6100), 303 (12 100). μ_{eff} = 4.65 BM. Soluble in DMSO (Λ_M = 13 mho cm^2 mol^{-1}, in 1 mM DMSO solution), DMF and acetone.

4.2.2. [Co(tolf)$_2$(bipy)(MeOH)$_2$], **2**

Tolfenamic acid (0.5 mmol, 131 mg) was dissolved in methanol (15 mL) followed by the addition of KOH (0.5 mmol, 28 mg). After 1 h stirring, the solution was added slowly, and simultaneously with a methanolic solution of bipy (0.25 mmol, 39 mg), to a methanolic solution (10 mL) of $CoCl_2 \cdot 6H_2O$ (0.25 mmol, 59 mg) and stirred for 30 min. The solution was left for slow evaporation. Rose-colored crystals [Co(tolf)$_2$(bipy)(MeOH)$_2$], **2** (130 mg, 65%) suitable for X-ray structure determination, was deposited after ten days. *Anal.* Calcd. for $C_{40}H_{38}CoCl_2N_4O_6$ (MW = 800.61) C, 60.01; H, 4.78; N, 7.00%; found: C, 59.94; H, 4.99; N, 6.66%. IR: ν_{max}, cm^{-1}; $\nu_{asym}(CO_2)$: 1583 (vs); $\nu_{sym}(CO_2)$: 1385 (vs); $\Delta = \nu_{asym}(CO_2) - \nu_{sym}(CO_2)$: 198 cm^{-1} (KBr disk); UV–vis: λ, nm (ε/M^{-1} cm^{-1}) as nujol mull: 690, 545, 480, 393, 346, 310; in DMSO: 680 (10), 540(25), 470 (25), 385 (210), 346 (2500), 309 (10 200). μ_{eff} = 4.73 BM. Soluble in DMSO (Λ_M = 8 mho cm^2 mol^{-1}, in 1 mM DMSO solution) and DMF.

4.2.3. [Co(tolf)$_2$(phen)(MeOH)$_2$], **3**

Complex **3** was prepared by the addition of a methanolic solution (15 mL) of Htolf (0.4 mmol, 105 mg) and KOH (0.4 mmol, 22 mg), which was stirred for 30 min, and of a methanolic solution of phen (0.2 mmol, 36 mg) to a methanolic solution (10 mL) of $CoCl_2 \cdot 6H_2O$ (0.2 mmol, 48 mg). The orange microcrystalline product of [Co(tolf)$_2$(phen)(MeOH)$_2$], **3** (105 mg, 65%) was collected after a few days. *Anal.* Calcd. for $C_{42}H_{38}CoCl_2N_4O_6$ (MW = 824.63) C, 61.17; H, 4.65; N, 6.79%; found C, 61.50; H, 4.72; N, 6.52%. IR: ν_{max}, cm^{-1}; $\nu_{asym}(CO_2)$: 1583 (vs); $\nu_{sym}(CO_2)$: 1384 (vs); $\Delta = \nu_{asym}(CO_2) - \nu_{sym}(CO_2)$: 199 cm^{-1} (KBr disk); UV–vis: λ, nm (ε, M^{-1} cm^{-1}) as nujol mull: 705, 565, 480, 393, 347, 308; in DMSO: 697 (10), 555 (40), 481 (35), 387 (290), 350 (4500), 308 (11 800). μ_{eff} = 4.75 BM. Soluble in DMSO (Λ_M = 11 mho cm^2 mol^{-1}, in 1 mM DMSO solution), DMF and $CHCl_3$.

4.2.4. [Co(tolf)$_2$(bipyam)], **4**

A solution (15 mL) of Htolf (0.6 mmol, 157 mg) and KOH (0.6 mmol, 33 mg) in MeOH was added after 1 h stirring simultaneously with a methanolic solution (10 mL) of bipyam (0.3 mmol, 52 mg) into a methanolic solution (10 mL) of $CoCl_2 \cdot 6H_2O$ (0.3 mmol, 72 mg) and the reaction mixture was stirred for 20 min and left for slow evaporation. Rose-colored crystals [Co(tolf)$_2$(bipyam)], **4** (155 mg, 70%) suitable for X-ray structure determination, were deposited after a week. *Anal.* Calcd. for $C_{38}H_{31}CoCl_2N_5O_4$ (MW = 751.54) C, 60.73; H, 4.16; N, 9.32%; found: C, 60.25; H, 4.14; N, 9.16%. IR: ν_{max}, cm^{-1}; $\nu_{asym}(CO_2)$, 1573 (vs); $\nu_{sym}(CO_2)$, 1402 (vs); $\Delta = \nu_{asym}(CO_2) - \nu_{sym}(CO_2)$: 171 cm^{-1} (KBr disk); UV–vis: λ, nm (ε, M^{-1} cm^{-1}) as nujol mull: 710, 554, 490, 392, 350, 312; in DMSO: 695 (10), 545 (60), 485 (40), 389 (215), 347 (6000), 310 (13 400). μ_{eff} = 4.25 BM. Soluble in DMSO (Λ_M = 11 mho cm^2 mol^{-1}, in 1 mM DMSO solution), DMF, $CHCl_3$ and CH_2Cl_2.

4.2.5. [Co(tolf)$_2$(py)$_2$(MeOH)$_2$], **5**

The complex was prepared by the addition of a methanolic solution (10 mL) of Htolf (0.5 mmol, 131 mg) and KOH (0.5 mmol, 28 mg), after 1 h of stirring, to a methanolic solution (10 mL) of $CoCl_2 \cdot 6H_2O$ (0.25 mmol, 59 mg) followed by the addition of 1.5 mL of pyridine. A red-brownish microcrystalline product of [Co(tolf)$_2$(py)$_2$(MeOH)$_2$], **5** (120 mg, 60%) was collected after a fortnight. *Anal.* Calcd. for $C_{40}H_{40}CoCl_2N_4O_6$ (MW = 802.62) C, 59.71; H, 5.26; N, 6.96%; found C, 60.15; H, 5.24; N, 7.24%. IR: ν_{max}, cm^{-1}; $\nu_{asym}(CO_2)$: 1582 (vs); $\nu_{sym}(CO_2)$: 1387 (vs); $\Delta = \nu_{asym}(CO_2) - \nu_{sym}(CO_2)$: 195 cm^{-1} (KBr disk); UV–vis: λ, nm (ε, M^{-1} cm^{-1}) as nujol mull: 703, 560, 485, 393, 351, 312; in DMSO: 695 (15), 565 (50), 480 (40), 385 (240), 348 (5400), 308 (14 600). μ_{eff} = 4.55 BM. Soluble in DMSO (Λ_M = 5 mho cm^2 mol^{-1}, in 1 mM DMSO solution), DMF, $CHCl_3$ and CH_2Cl_2.

4.3. DNA-binding studies

The interaction of tolfenamic acid and complexes **1**–**5** with CT DNA has been studied with UV spectroscopy in order to investigate the possible binding modes to CT DNA and to calculate the binding constants to CT DNA (K_b). In UV titration experiments, the spectra of CT DNA in the presence of each compound have been recorded for a constant CT DNA concentration in diverse [compound]/[CT DNA] mixing ratios (r). The binding constants, K_b, of the compounds with CT DNA have been determined using the UV spectra of the compound recorded for a constant concentration in the absence or presence of CT DNA for diverse r values. Control experiments with DMSO were performed and no changes in the spectra of CT DNA were observed.

Viscosity experiments were carried out using an ALPHA L Fungilab rotational viscometer equipped with an 18 mL LCP spindle and the measurements were performed at 100 rpm. The viscosity of a DNA solution has been measured in the presence of increasing amounts of Htolf or complexes **1**–**5**. The relation between the relative solution viscosity (η/η_0) and DNA length (L/L_0) is given by the equation $L/L_0 = (\eta/\eta_0)^{1/3}$, where L_0 denotes the apparent molecular length in the absence of the compound [15]. The obtained data are presented as $(\eta/\eta_0)^{1/3}$ versus r, where η is the viscosity of DNA in the presence of a compound, and η_0 is the viscosity of DNA alone in buffer solution.

The interaction of complexes **1**–**5** with CT DNA has been also investigated by monitoring the changes observed in the cyclic voltammogram of a 0.40 mM 1:2 DMSO:buffer solution of complex upon addition of CT DNA at diverse r values. The buffer was also

used as the supporting electrolyte and the cyclic voltammograms were recorded at $\nu = 100$ mV s^{-1}.

The competitive studies of each compound with EB have been investigated by fluorescence spectroscopy in order to examine whether the compound can displace EB from its CT DNA-EB complex. The CT DNA-EB complex was prepared by adding 20 μM EB and 26 μM CT DNA in buffer (150 mM NaCl and 15 mM trisodium citrate at pH 7.0). The intercalating effect of Htolf and complexes **1**–**5** with the DNA-EB complex was studied by adding a certain amount of a solution of the compound step by step into the solution of the DNA-EB complex. The influence of the addition of each compound to the DNA-EB complex solution has been obtained by recording the variation of fluorescence emission spectra.

4.4. Albumin binding studies

The protein binding study was performed by tryptophan fluorescence quenching experiments using bovine (BSA, 3 μM) or human serum albumin (HSA, 3 μM) in buffer (containing 15 mM trisodium citrate and 150 mM NaCl at pH 7.0). The quenching of the emission intensity of tryptophan residues of BSA at 343 nm or HSA at 351 nm was monitored using Htolf or complexes **1**–**5** as quenchers with increasing concentration [53]. Fluorescence spectra were recorded in the range 300–500 nm at an excitation wavelength of 295 nm. The fluorescence spectra of tolfenamic acid and its complexes were recorded under the same experimental conditions and a maximum emission appeared at 330 nm. Therefore, the quantitative studies of the serum albumin fluorescence spectra were performed after their correction by subtracting the spectra of the compounds.

4.5. X-ray structure determination

Single-crystal X-ray diffraction data were collected at room temperature (**2**) and 150 K (**4**) on a Nonius Kappa CCD diffractometer using graphite monochromated Mo-Kα radiation ($\lambda = 0.71073$ Å). The data were processed using DENZO [54]. The structures were solved by direct methods implemented in SIR97 [55] and refined by a full-matrix least-squares procedure based on F^2 with SHELXL-97 [56]. All the non-hydrogen atoms were refined anisotropically. All the hydrogen atoms were readily located in difference Fourier maps and were subsequently treated as riding atoms in geometrically idealized positions with $U_{iso}(H) = kU_{eq}$(C or N), where $k = 1.5$ for NH and methyl groups, which were permitted to rotate but not to tilt, and 1.2 for all other H atoms. Hydrogen atom bonded to methanol O atom (**2**) was refined freely. The Flack parameter for **2** converged to 0.47(2) suggesting that the complex is a racemic twin with the ratio of enantiomers 0.53:0.47. Crystallographic data are listed in Table 8.

Acknowledgements

Financial support from the Slovenian Research Agency (ARRS) through project P1-0175 is gratefully acknowledged.

Appendix. Supplementary material

Supplementary data related to this article can be found online at doi:10.1016/j.ejmech.2011.12.004.

References

[1] P.V. Bernhardt, G.A. Lawrance, in: J.A. McCleverty, T.J. Meyer (Eds.), Comprehensive Coordination Chemistry II, vol. 6, 2003, pp. 1–45 ch. 1.
[2] P.J. Sadler, Adv. Inorg. Chem. 36 (1991) 1–48.
[3] M.D. Hall, T.W. Failes, N. Yamamoto, T.W. Hambley, Dalton Trans. (2007) 3983–3990.
[4] N. Hadjiliadis, E. Sletten (Eds.), Metal Complex – DNA Interactions, John Wiley & Sons, Inc., Hoboken, NJ, 2009 and the references therein.
[5] H. Lopez-Sandoval, M.E. Londono-Lemos, R. Garza-Velasco, I. Poblano-Melendez, P. Granada-Macias, I. Gracia-Mora, N. Barba-Behrens, J. Inorg. Biochem. 102 (2008) 1267–1276.
[6] I. Ott, A. Abraham, P. Schumacher, H. Shorafa, G. Gastl, R. Gust, B. Kircher, J. Inorg. Biochem. 100 (2006) 1903–1906.
[7] R. Eshkourfu, B. Cobeljic, M. Vujcic, I. Turel, A. Pevec, K. Sepcic, M. Zec, S. Radulovic, T. Srdic-Radic, D. Mitic, K. Andjelkovic, D. Sladic, J. Inorg. Biochem. 105 (2011) 1196–1203.
[8] D.U. Miodragovic, G.A. Bogdanovic, Z.M. Miodragovic, M.D. Radulovic, S.B. Novakovic, G.N. Kaludjerovic, H. Kozlowski, J. Inorg. Biochem. 100 (2006) 1568–1574.
[9] K. Nomiya, A. Yoshizawa, K. Tsukagoshi, N.C. Kasuga, S. Hirakawa, J. Watanabe, J. Inorg. Biochem. 98 (2004) 46–60.
[10] E.K. Efthimiadou, A. Karaliota, G. Psomas, Bioorg. Med. Chem. Lett. 18 (2008) 4033–4037.
[11] J. Lv, T. Liu, S. Cai, X. Wang, L. Liu, Y. Wang, J. Inorg. Biochem. 100 (2006) 1888–1896.
[12] Z. Weiqun, Y. Wen, X. Liqun, C. Xianchen, J. Inorg. Biochem. 99 (2005) 1314–1319.
[13] A. Bottcher, T. Takeuchi, K.I. Hardcastle, T.J. Meade, H.B. Gray, Inorg. Chem. 36 (1997) 2498–2504.
[14] T. Takeuchi, A. Bottcher, C.M. Quezada, T.J. Meade, H.B. Gray, Bioorg. Med. Chem. 7 (1999) 815–819.
[15] F. Dimiza, A.N. Papadopoulos, V. Tangoulis, V. Psycharis, C.P. Raptopoulou, D.P. Kessissoglou, G. Psomas, Dalton Trans. 39 (2010) 4517–4528.
[16] F. Dimiza, A.N. Papadopoulos, V. Tangoulis, V. Psycharis, C.P. Raptopoulou, D.P. Kessissoglou, G. Psomas, J. Inorg. Biochem. 107 (2012) 54–64.
[17] C.P. Duffy, C.J. Elliott, R.A. O'Connor, M.M. Heenan, S. Coyle, I.M. Cleary, K. Kavanagh, S. Verhaegen, C.M. O'Loughlin, R. NicAmhlaoibh, M. Clynes, Eur. J. Cancer 34 (1998) 1250–1259.
[18] A.R. Amin, P. Vyas, M. Attur, J. Leszczynskapiziak, I.R. Patel, G. Weissmann, S.B. Abramson, Proc. Natl. Acad. Sci. 92 (1995) 7926–7930.
[19] W.J. Wechter, E.D. Murray, D. Kantoci, D.D. Quiggle, D.D. Leipold, K.M. Gibson, J.D. McCracken, Life Sci. 66 (2000) 745–753.
[20] K. Kim, J. Yoon, J.K. Kim, S.J. Baek, T.E. Eling, W.J. Lee, J. Ryu, J.G. Lee, J. Lee, J. Yoo, Biochem. Biophys. Res. Commun. 325 (2004) 1298–1303.
[21] G. Ribeiro, M. Benadiba, A. Colquhoun, D. de Oliveira Silva, Polyhedron 27 (2008) 1131–1137.
[22] T. Zhang, T. Otevrel, Z.Q. Gao, Z.P. Gao, S.M. Ehrlich, J.Z. Fields, B.M. Boman, Cancer Res. 61 (2001) 8664–8667.
[23] S. Roy, R. Banerjee, M. Sarkar, J. Inorg. Biochem. 100 (2006) 1320–1331.
[24] G. Crisponi, V.M. Nurchi, D. Fanni, C. Gerosa, S. Nemolato, G. Faa, Coord. Chem. Rev. 254 (2010) 876–889.
[25] J.A. Drewry, P.T. Gunning, Coord. Chem. Rev. 255 (2011) 459–472.
[26] J.E. Weder, C.T. Dillon, T.W. Hambley, B.J. Kennedy, P.A. Lay, J.R. Biffin, H.L. Regtop, N.M. Davies, Coord. Chem. Rev. 232 (2002) 95–126 and references therein.
[27] E. Moilanen, H. Kankaanranta, Pharmacol. Toxicol. 75 (Suppl. II) (1994) 60.
[28] D. Kovala-Demertzi, N. Kourkoumelis, A. Koutsodimou, A. Moukarika, E. Horn, E.R.T. Tiekink, J. Organom. Chem. 620 (2001) 194–201.
[29] D. Kovala-Demertzi, A. Galani, M.A. Demertzis, S. Skoulika, C. Kotoglou, J. Inorg. Biochem. 98 (2004) 358–364.
[30] A. Tarushi, G. Psomas, C.P. Raptopoulou, D.P. Kessissoglou, J. Inorg. Biochem. 103 (2009) 898–905.
[31] A. Tarushi, C.P. Raptopoulou, V. Psycharis, A. Terzis, G. Psomas, D.P. Kessissoglou, Bioorg. Med. Chem. 18 (2010) 2678–2685.
[32] K.C. Skyrianou, F. Perdih, I. Turel, D.P. Kessissoglou, G. Psomas, J. Inorg. Biochem. 104 (2010) 161–170.
[33] K.C. Skyrianou, F. Perdih, I. Turel, D.P. Kessissoglou, G. Psomas, J. Inorg. Biochem. 104 (2010) 740–749.
[34] K.C. Skyrianou, V. Psycharis, C.P. Raptopoulou, D.P. Kessissoglou, G. Psomas, J. Inorg. Biochem. 105 (2011) 63–74.
[35] A. Tarushi, E. Polatoglou, J. Kljun, I. Turel, G. Psomas, D.P. Kessissoglou, Dalton Trans. 40 (2011) 9461–9473.
[36] K.C. Skyrianou, F. Perdih, A.N. Papadopoulos, I. Turel, D.P. Kessissoglou, G. Psomas, J. Inorg. Biochem. 105 (2011) 1273–1285.
[37] P. Christofis, M. Katsarou, A. Papakyriakou, Y. Sanakis, N. Katsaros, G. Psomas, J. Inorg. Biochem. 99 (2005) 2197–2210.
[38] F. Dimiza, S. Fountoulaki, A.N. Papadopoulos, C.A. Kontogiorgis, V. Tangoulis, C.P. Raptopoulou, V. Psycharis, A. Terzis, D.P. Kessissoglou, G. Psomas, Dalton Trans. 40 (2011) 8555–8568.
[39] F. Dimiza, F. Perdih, V. Tangoulis, I. Turel, D.P. Kessissoglou, G. Psomas, J. Inorg. Biochem. 105 (2011) 476–489.
[40] S. Fountoulaki, F. Perdih, I. Turel, D.P. Kessissoglou, G. Psomas, J. Inorg. Biochem. 105 (2011) 1645–1655.
[41] K. Nakamoto, Infrared and Raman Spectra of Inorganic and Coordination Compounds, Part B: Applications in Coordination, Organometallic, and Bioinorganic Chemistry, sixth ed. Wiley, New Jersey, 2009.
[42] C. Tan, J. Liu, H. Li, W. Zheng, S. Shi, L. Chen, L. Ji, J. Inorg. Biochem. 102 (2008) 347–358.

[43] Y. Wang, H. Zhang, G. Zhang, W. Tao, S. Tang, J. Luminescence 126 (2007) 211–218.
[44] V. Rajendiran, R. Karthik, M. Palaniandavar, H. Stoeckli-Evans, V.S. Periasamy, M.A. Akbarsha, B.S. Srinag, H. Krishnamurthy, Inorg. Chem. 46 (2007) 8208–8221.
[45] S. Roy, R. Banerjee, M. Sarkar, J. Inorg. Biochem. 100 (2006) 1320–1331.
[46] Q. Zhang, J. Liu, H. Chao, G. Xue, L. Ji, J. Inorg. Biochem. 83 (2001) 49–55.
[47] A.M. Pyle, J.P. Rehmann, R. Meshoyrer, C.V. Kumar, N.J. Turro, J.K. Barton, J. Am. Chem. Soc. 111 (1989) 3053–3063.
[48] A. Dimitrakopoulou, C. Dendrinou-Samara, A.A. Pantazaki, M. Alexiou, E. Nordlander, D.P. Kessissoglou, J. Inorg. Biochem. 102 (2008) 618–628.
[49] G. Psomas, J. Inorg. Biochem. 102 (2008) 1798–1811.
[50] J.L. Garcia-Gimenez, M. Gonzalez-Alvarez, M. Liu-Gonzalez, B. Macias, J. Borras, G. Alzuet, J. Inorg. Biochem. 103 (2009) 923–934.
[51] J.L. Garcia-Gimenez, G. Alzuet, M. Gonzalez-Alvarez, M. Liu-Gonzalez, A. Castineiras, J. Borras, J. Inorg. Biochem. 103 (2009) 243–255.
[52] D. Li, J. Tian, W. Gu, X. Liu, S. Yan, J. Inorg. Biochem. 104 (2010) 171–179.
[53] J.R. Lakowicz, Principles of Fluorescence Spectroscopy, third ed. Springer, New York, 2006.
[54] Z. Otwinowski, W. Minor, Methods in Enzymology, in: C.W. CarterJr., R.M. Sweet (Eds.), Macromolecular Crystallography, Part A, vol. 276, Academic Press, New York, 1997, pp. 307–326.
[55] A. Altomare, M.C. Burla, M. Camalli, G.L. Cascarano, C. Giacovazzo, A. Guagliardi, A.G.G. Moliterni, G. Polidori, R. Spagna, J. Appl. Crystallogr. 32 (1999) 115–119.
[56] G.M. Sheldrick, SHELXL-97, Program for the Refinement of Crystal Structures, University of Göttingen, Germany, 1997.